



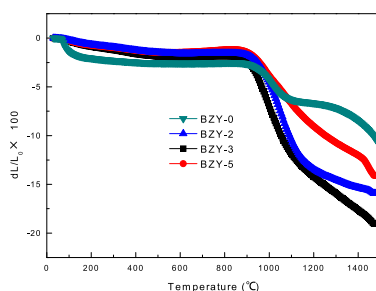
Short communication

Sintering and electrochemical performance of Y_2O_3 -doped barium zirconate with Bi_2O_3 as sintering aidsShiru Le^a, Jing Zhang^b, Xiaodong Zhu^a, Jingru Zhai^c, Kening Sun^{a,*}^a Natural Science Research Center, Academy of Fundamental and Interdisciplinary Sciences, Harbin Institute of Technology, Harbin, Heilongjiang 150080, China^b China Faw Group Corporation R&D Center, Material Department Surface Protection Research Sec., No. 3013 Heping Street, Changchun, Jilin 130011, China^c Applied Chemistry Department, College of Science, Harbin Institute of Technology, Harbin, Heilongjiang 150001, China

HIGHLIGHTS

- ▶ Bi_2O_3 as sintering aid for BZY was evaluated.
- ▶ The activation energy for densification is 5.40 eV for BZY-3.
- ▶ The conductivity is $1.13 \times 10^{-3} \text{ S cm}^{-1}$ for BZY-2 sintered at 1400 °C for 24 h.
- ▶ The OCV is 0.95 V with the ionic transport number of 0.83 at 600 °C.

GRAPHICAL ABSTRACT



ARTICLE INFO

Article history:

Received 9 October 2012

Received in revised form

5 January 2013

Accepted 13 January 2013

Available online 19 January 2013

Keywords:

Solid oxide fuel cells

Yttria-doped barium zirconate

Bismuth oxide

Sintering aids

ABSTRACT

Decreasing Y_2O_3 -doped barium zirconate (BZY) sintering temperature is crucial for its implementation in solid oxide fuel cells (SOFC). Bismuth oxide as sintering aid for BZY is evaluated. It is found that 3 mol% Bi_2O_3 doped BZY (BZY-3) improves its shrinkage from 10.4% to 19.02% at about 1480 °C, with the maximum shrinkage rate increasing from $-0.20 \text{ mm min}^{-1}$ to $-0.34 \text{ mm min}^{-1}$. The activation energy for densification is 5.40 eV for BZY-3. The SEM images confirms that it is porous for BZY without Bi_2O_3 (BZY-0), but that less small pores could be seen for BZY-3 and 5 mol% Bi_2O_3 doped BZY (BZY-5) sintered at 1400 °C for 24 h. Bi_2O_3 addition decreases the grain boundary conductivity for BZY-3 and BZY-5 obviously, but is less significant for BZY-2. It is $1.13 \times 10^{-3} \text{ S cm}^{-1}$ for BZY-2 in wet hydrogen atmosphere at 600 °C sintered at 1400 °C for 24 h, nearly equal to that of BZY-0. The open circuit voltage is 0.95 V, with the ionic transport number of 0.83 for BZY-2 under SOFC operating conditions.

© 2013 Elsevier B.V. All rights reserved.

1. Introduction

Low valence element-doped alkaline earth metal zirconate exhibit high conductivity and good chemical stability [1]. These materials are promising candidates as electrolytes in solid oxide fuel cells. Of all the members of alkaline earth metal zirconates, Y_2O_3 doped BaZrO_3 (BZY) are an important class of proton conductors due to their high protonic conductivity [2] and high chemical stability in SOFC operating atmospheres [3]. In addition,

BZY exhibits higher bulk conductivity than that of doped BaCeO_3 [4,5].

The refractory nature of BZY leads to significant challenges to its implementation in fuel cells and other devices is that it needs high sintering temperature (typically 1700–1800 °C) and long sintering time (24 h) [5–7]. Not only are these conditions energy consuming, but that they are incompatible with most potential electrode materials and thereby preclude the fabrication of co-sintered structures [1].

Most of the transition metal oxides are effective sintering aids for perovskite-type protonic conductors. For example, $\text{BaZr}_{0.85}\text{Y}_{0.15}\text{O}_{3-\delta}$, modified with 4 mol% ZnO, achieves full density at a sintering

* Corresponding author. Tel./fax: +86 451 8641 2153.

E-mail address: keningsun@yahoo.com.cn (K. Sun).

temperature between 1350 °C for 4 h [8]. However, Babilo et al. [9] observed that the addition of ZnO lower the bulk conductivity, which is probably the formation of strong proton trapping at Zn_{Zr}'' .

The addition of bismuth oxide can effectively produce single phase perovskite $\text{Bi}_{0.5}\text{Na}_{0.5}\text{ZrO}_3$, and effectively improved its density [10]. Bi_2O_3 aids the 10ScSZ sintering processes and allows the samples to sinter at lower temperature [11]. But Duval observed that minor element addition (<2 mol%) of TiO_2 , MgO , Mo , Al_2O_3 and Bi_2O_3 do not contribute to any improvement of the sintering behavior [12].

In this work, the sintering performance of the $\text{BaZr}_{0.90}\text{Y}_{0.10}\text{O}_{3-\delta}$ with the addition of Bi_2O_3 as sintering aid and its electrochemical performance was evaluated, together with its open circuit voltage when using it as electrolyte under SOFC operating conditions. The activation energy for densification with Bi_2O_3 as sintering aid was calculated.

2. Experimental methods

The $\text{BaZr}_{0.90}\text{Y}_{0.10}\text{O}_{3-\delta}$ (BZY) powders were synthesized via a chemical solution route in which high purity $\text{Ba}(\text{NO}_3)_2$, $\text{Y}(\text{NO}_3)_3 \cdot 6\text{H}_2\text{O}$, and $\text{ZrO}(\text{NO}_3)_2 \cdot 2\text{H}_2\text{O}$ were used as the precursor reagents and ethylene diamine tetraacetic acid (EDTA) and citric acid served as chelating agents. After dissolution of the nitrates into de-ionized water, EDTA and NH_4OH were added into the solution with the NH_4OH adjusted to obtain a pH from 8 to 10. The solvents were removed upon heat treatment at 100 °C for over 24 h. Then these were calcined at selected temperature for 5 h in air to obtain BZY powder. The powders were mixed with 0 mol%, 2 mol%, 3 mol% and 5 mol% Bi_2O_3 , respectively, and milled at a planetary mill for at least 48 h. These were denoted as BZY-0, BZY-2, BZY-3, BZY-5, respectively. The powder were cold pressed at 300 MPa for 20 min to obtain dense primarily pellets samples. Then there were sintered at 1400 °C for 24 h under the cover of BZY powder in air conditions.

X-ray diffraction (XRD) spectra of the powders were collected at room temperature using an XRD (Rigachu D/max 2500 V/PC, Tokyo, Japan) with Cu K α radiation. The phases were identified with JADE5.0 software. The dilatometry experiments were performed using samples with powders calcined at 1200 °C for 5 h in a dilatometer (Netzsch DIL 402 PC, Germany). Data were collected at a heating rate of 5 °C min⁻¹, 10 °C min⁻¹, 15 °C min⁻¹ in an air atmosphere.

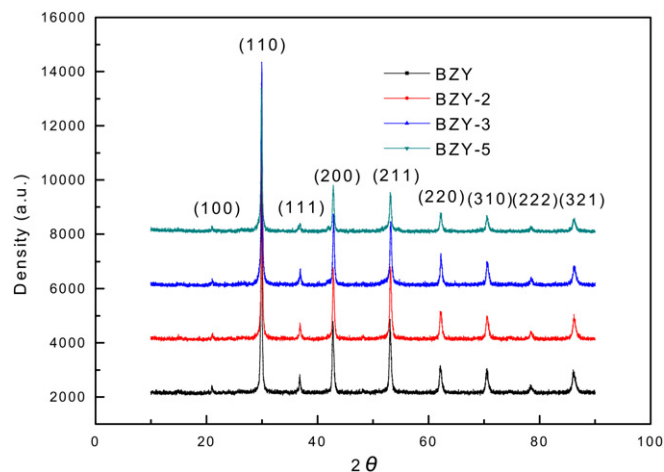


Fig. 2. XRD patterns of BZY pellets with various amount of Bi_2O_3 sintered at 1400 °C for 24 h.

The surface microstructure of the pellets was observed using HITACHI 8000. In order to perform electrical characterization of the samples which sintered at 1400 °C for 24 h, Pt paste was painted on both sides of the specimens, dried and fired at 800 °C for 30 min. The conductivity of the sintered pellets was measured by AC impedance spectroscopy using M2273 under hydrogen with 3% H_2O atmosphere in frequency range of 100 mHz–100 MHz. The resulting impedance spectra were analyzed using the software package Zview.

Open circuit voltage (OCV) measurements were collected under fuel cell conditions to evaluate the ionic transport number of the materials in an Arbin Instrument. For this purpose, porous Pt electrodes were pasted onto both sides of the sintered BZY-2 disk with 10.5 mm in diameter and 0.8 mm in thickness. Voltage was generated by exposing one side to hydrogen with 3% H_2O and the other side to oxygen in an alumina oxide tube. The ionic transport number was calculated from the ratio of the measured OCV to the theoretical voltage

$$t_{\text{ion}} = \frac{\text{OCV}}{E_{\text{th}}}$$

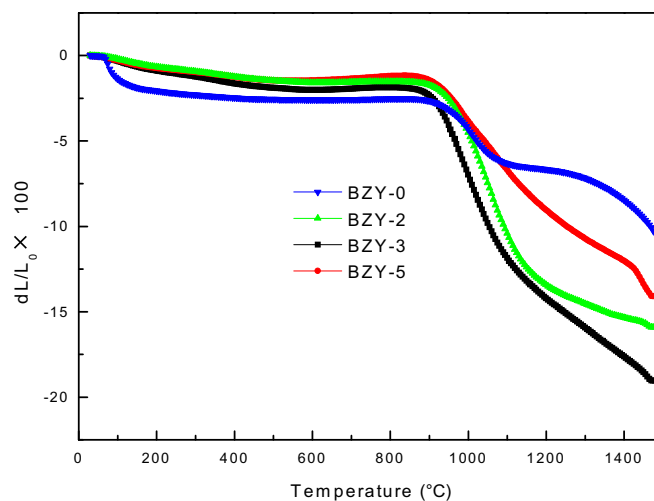


Fig. 3. Dilatometric curves of BZY with various amount of Bi_2O_3 .

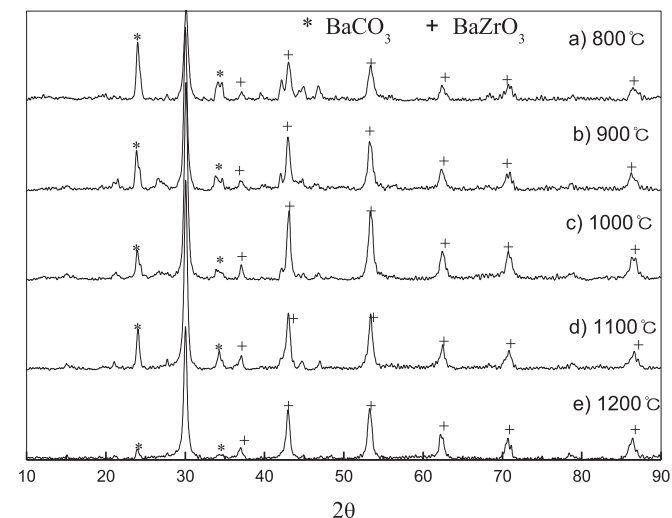


Fig. 1. X-ray diffraction patterns of powders calcined at a) 800 °C, b) 900 °C, c) 1000 °C, d) 1100 °C, e) 1200 °C.

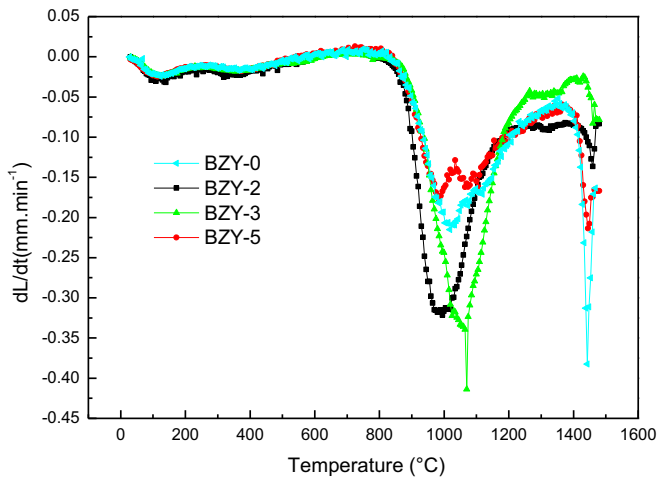


Fig. 4. The shrinkage rate of BZY with various amount of Bi_2O_3 .

3. Results and discussions

The X-ray powder diffraction patterns of powders calcined at various temperatures between 800 °C and 1200 °C was shown in Fig. 1. It indicated that the precursor materials were composed primarily of the cubic perovskite phase, with the carbonate barium occurring. Pure BaZrO_3 is primitive cubic perovskite, group Pm3m. With the introduction of Y^{3+} ions (0.93 Å) at the B-sites (0.80 Å for Zr^{4+}), the BO_6 polyhedra may tilt and distort thus causing distortion of the lattice. The peaks in $41^\circ \sim 45^\circ$ split at low calcined temperature was contributed to the presence of tetragonal structure [13].

The carbonate barium decreased as the calcination temperature increased. The XRD patterns of BZY pellets with various amount of Bi_2O_3 sintered at 1400 °C for 24 h was presented in Fig. 2. All specimens were cubic, regardless of the addition of Bi_2O_3 , and no carbonate barium peaks could be observed.

Figs. 3 and 4 showed the shrinkage and its rate of the BZY with various amount of Bi_2O_3 as sintering aids. Dual [14] observed that 1.5 mol% Bi_2O_3 addition did not contribute to any improvement of the BZY sintering behavior. However, in our experiment in Fig. 3 indicated that the shrinkage of BZY-0 was 10.4% at 1480 °C, while it increased to 19.02% at 1470 °C for BZY-3, then it decreased to 14.6% for BZY-5. The shrinkage rate presented in Fig. 4 showed that the maximum shrinkage increased from $-0.20 \text{ mm min}^{-1}$ at about 1000 °C for BZY-0 to $-0.34 \text{ mm min}^{-1}$ for BZY-3. The SEM images in Fig. 5 confirmed that it is porous for BZY-0, but that less small pores could be seen for BZY-3 and BZY-5 sintered at 1400 °C for 24 h. This was because Bi_2O_3 facilitated the atom diffusion along grain boundary, therefore improved the shrinkage performance [15]. It was evident that the addition of small amount Bi_2O_3 can effectively improve its densification. However, too high content of sintering aid is detrimental for its densification. This was also observed by Tao [18] and Wang [16] using ZnO as sintering aid. Wang [17] revealed that $\text{BaO} \cdot \text{ZnO}$ eutectic, rather than ZnO, was responsible for the densification.

Starting from Herring's general flux equation [18], the following equation can be obtained

$$\ln(-dL/Ldt) = \ln\left(\frac{\gamma Q \Gamma D_0}{RT}\right) - n \ln d - Q/RT \quad (1)$$

Here, γ is the surface energy, Q is the atomic volume, and δ is the grain boundary thickness, L is the actual length, d is the actual grain

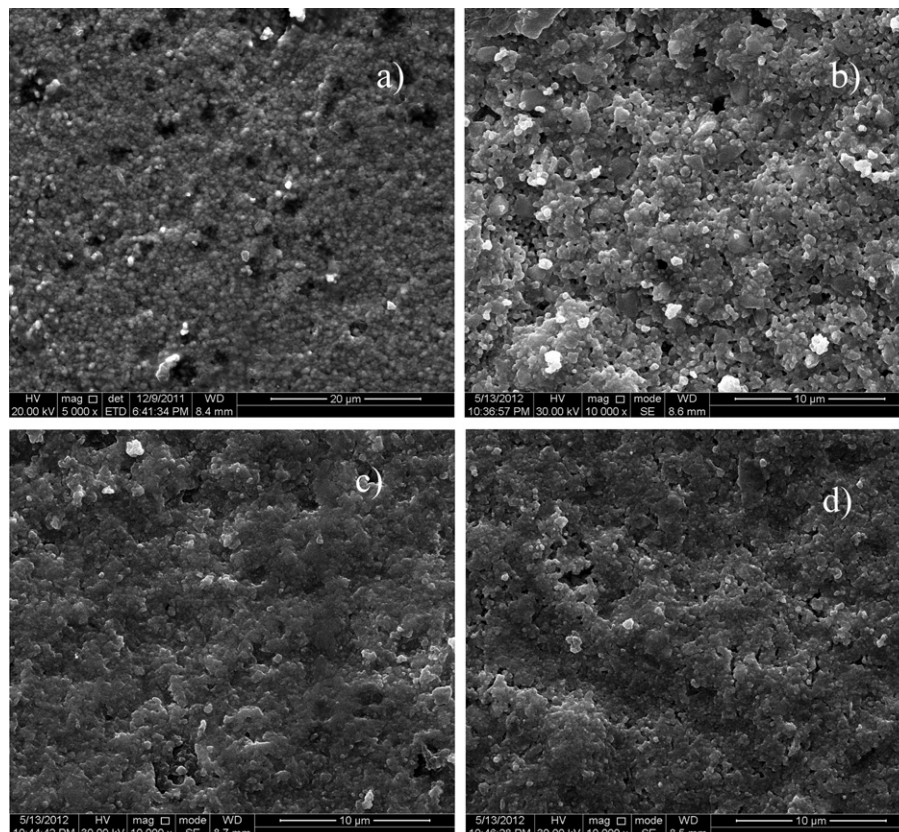


Fig. 5. SEM surface images of the samples sintered at 1400 °C for 24 h. a) BZY-0, b) BZY-2, c) BZY-3 d) BZY-5.

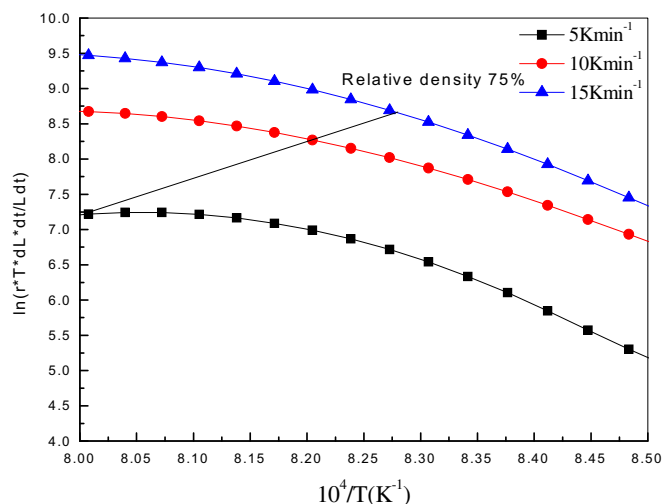


Fig. 6. The activation energy for densification determination curves of BZY-3.

size, R is the Boltzmann constant, T is the current temperature, and Q is the activation energy. The activation energy of the densification can be determined by simply plotting the term on the left-hand side of Eq. (1) versus $1/T$ at a constant relative density for different heating rates. The slope of the obtained straight line equals $-Q/R$. The activation was determined from the slope of the line at various heating rate [19]. The temperature range of 900–1000 °C was chosen, as the sample was in its fast densification process, which could be seen from Figs. 3 and 4.

The densification activation determination curves of BZY-3 were shown in Fig. 6. It was 5.40 eV for BZY-3 during densification.

The EIS spectroscopy of the BZY with various amount of Bi_2O_3 content in temperature range of 500–800 °C were shown in Fig. 7.

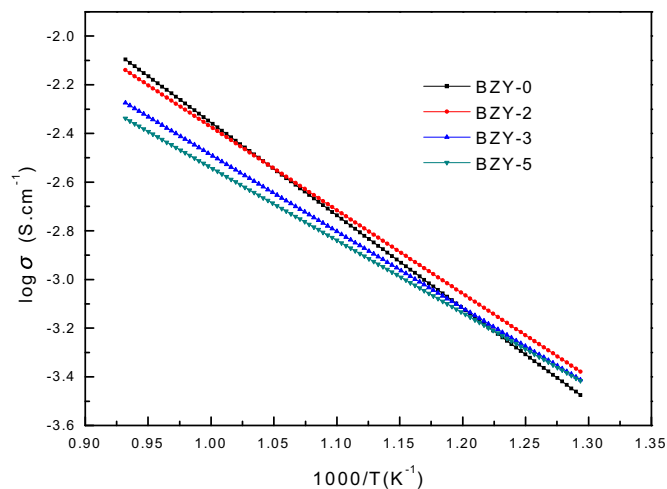


Fig. 8. The conductivity of the samples sintered at 1400 °C for 24 h.

The respective conductivities were deduced from the resistance terms obtained from the impedance data by accounting for the sample geometry according to Eq (2).

$$\sigma = \frac{L}{AR_1 + R_2} \quad (2)$$

where L is the sample thickness and A is its area, R_1 and R_2 is the resistance of the bulk and of the grain boundary. The high frequency arc corresponds to phenomena occurring in the bulk of the electrolyte. The lower frequency impedance variation represents the behavior occurring at the electrode–electrolyte interface. The arc of the mid-frequency range can be assigned to grain boundary

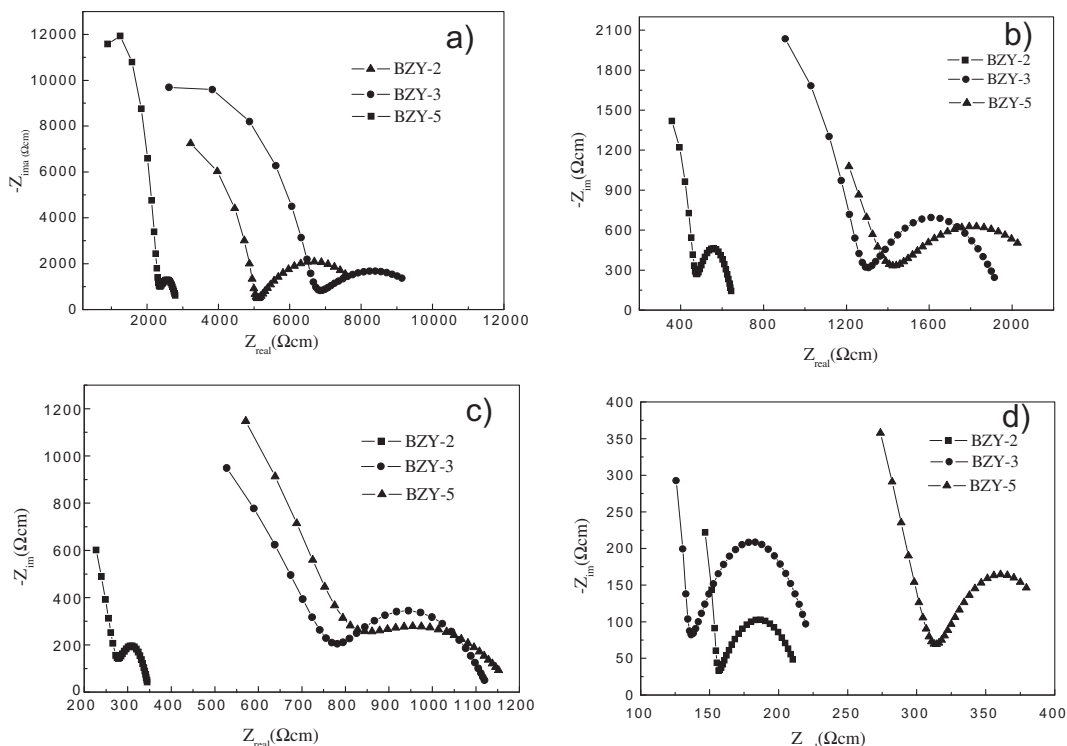


Fig. 7. Impedance spectroscopy of the samples sintered at 1400 °C for 24 h at a) 500 °C, b) 600 °C, c) 700 °C, d) 800 °C.

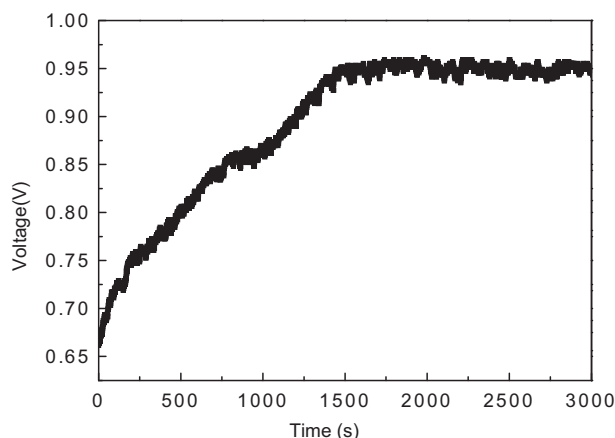


Fig. 9. The OCV of the cell using BZY-2 as electrolyte at 600 °C.

impedances. At temperature lower than 300 °C, the obtained capacity values for BZY oxide associated with bulk component were at least two orders of magnitude lower than that for grain boundary [20]. At temperature higher than 300 °C, the grain boundary and grain interior resistances can no longer be separated [21]. The equivalent circuit model for such materials typically involves (RQ) sub-circuits, where R, a resistor, and Q, a constant phase element are in parallel to one another.

The spectrum consists one large semicircle starting at the origin and a small semicircle at low frequency. Unlike the spectrum measured at low temperature (<300 °C), where bulk, grain boundary and electrode processes can be separated, the bulk and grain boundary contribution are strongly overlap in the spectrum at high temperature. Therefore, at high temperature, the total resistance can be determined from the high frequency intercept of the spectrum with the real axis [22].

At temperature higher than 500 °C, semi-circles arising from bulk and grain boundary resistances can not be resolved [23], and the total resistance determined from the impedance spectra is the sum of $R_{\text{total}} = R_{\text{bulk}} + R_{\text{grain boundary}}$ at the intercept of real axis [2]. In the wet state, protonic conduction dominate and suppress electron hole in the BZY over a wide range of P_{O_2} [22].

It demonstrated that the highest conductivity was that of BZY-2. But in temperature range of 550–800 °C, the conductivity of BZY-3 and BZY-5 was lower than that of BZY-0. This was because that Bi_2O_3 decreased the grain boundary conductivity. The calculated results of the conductivity were presented in Fig. 8. However, the conductivity of BZY-2 was $1.13 \times 10^{-3} \text{ S cm}^{-1}$ at 600 °C sintered at 1400 °C for 24 h. This was nearly equal to BZY-0 of $1.14 \times 10^{-3} \text{ S cm}^{-1}$. This demonstrated that small (<2 mol%) amount of Bi_2O_3 did not decrease the conductivity. The conductivity of $1.13 \times 10^{-3} \text{ S cm}^{-1}$ for BZY-2 at 600 °C was much higher than that of $\text{BaZr}_{0.95}\text{In}_{0.05}\text{O}_{3-\delta}$, which was $1.2 \times 10^{-4} \text{ S cm}^{-1}$ at 600 °C with the samples sintered at 1500–1650 °C for 10 h [24]. It was comparable with that of $\text{BaZr}_{0.90}\text{In}_{0.10}\text{O}_{3-\delta}$, which was $1.1 \times 10^{-3} \text{ S cm}^{-1}$ at 600 °C with the samples sintered at 1800 °C for 5 h in air [25].

To study the open circuit voltage (OCV) is important for BZY using as the SOFC electrolyte. The OCV of BZY-2 under hydrogen atmosphere containing 3 mol% H_2O as fuel and air as oxidant was shown in Fig. 9. Platinum pastes were used as anode and cathode in

both sides. The OCV increased slowly as the fuel flowed proceed because of the increase of oxygen concentration gradient increased. It was kept stable at about 0.95 V about 1500 s later, with the ionic transport number 0.83, compared with the theory value of 1.15 V for pure BZY electrolyte. The low ion transport number was attributed to the reduction of bismuth oxide to metal bismuth, which led to electronic conduction. This showed that bismuth oxide was detrimental to its open circuit voltage. The transport number was relatively small compared with 4 mol% ZnO doped BZY, which was 0.86 at 700 °C [9].

4. Conclusions

Bi_2O_3 as sintering aid for BZY was evaluated and found that it was effective to improve BZY shrinkage performance. 3 mol% Bi_2O_3 doped BZY improved its shrinkage from 10.4% to 19.02% at about 1480 °C, with the maximum shrinkage rate increasing from $-0.20 \text{ mm min}^{-1}$ to $-0.34 \text{ mm min}^{-1}$. The conductivity of BZY-2 was $1.13 \times 10^{-3} \text{ S cm}^{-1}$ at 600 °C sintered at 1400 °C for 24 h. The calculated activation energy for densification was 5.40 eV for BZY-3. The open circuit voltage is 0.95 V, with the ionic transport number is 0.83 under SOFC operating conditions.

Acknowledgments

This work was supported by National Scientific Foundation of China (No. 21006016), Specialized Research Fund for the Doctoral Program of Higher Education of China (20102302120044) and Postdoctoral Science-Research Foundation (LBH-Q11112).

References

- [1] Z.Z. Peng, R.S. Guo, Z.G. Yin, J. Li, J. Am. Ceram. Soc. 91 (2008) 1534–1538.
- [2] Z. Khani, M. Taillades-Jacquín, G. Taillades, M. Marrony, D.J. Jones, J. Roziere, J. Solid State Chem. 182 (2009) 790–798.
- [3] N.S. Fumitada Iguchi, Hiroo Yugami, J. Mater. Chem. 20 (2010) 6265–6270.
- [4] K.D. Kreuer, Solid State Ionics 125 (1999) 285–302.
- [5] E. Fabbri, D. Pergolesi, E. Traversa, Chem. Soc. Rev. 39 (2010) 4355–4369.
- [6] Y. Yamazaki, R. Hernandez-Sanchez, S.M. Haile, Chem. Mater. 21 (2009) 2755–2762.
- [7] F. Iguchi, N. Sata, T. Tsurui, H. Yugami, Solid State Ionics 178 (2007) 691–695.
- [8] Shanwen Tao, J.T.S. Irvine, Adv. Mater. 18 (2006) 1581–1584.
- [9] P. Babilo, S.M. Haile, J. Am. Ceram. Soc. 88 (2005) 2362–2368.
- [10] J. Jaiban Panupong, Sukanda, Anucha Watcharapason, ScienceAsia 37 (2011) 256–261.
- [11] B. Bai, N.M. Sammes, A.L. Smirnova, J. Power Sources 176 (2008) 76–81.
- [12] S.B.C. Duval, P. Holtappels, U. Stimming, T. Graule, Solid State Ionics 179 (2008) 1112–1115.
- [13] L. Malavasi, C. Ritter, G. Chiodelli, Chem. Mater. 20 (2008) 2343–2351.
- [14] S.B.C. Duval, P. Holtappels, U. Stimming, T. Graule, Solid State Ionics 179 (2008) 1112–1115.
- [15] J.D. Nicholas, L.C. De Jonghe, Solid State Ionics 178 (2007) 1187–1194.
- [16] Y.Z. Wang, A. Chesnaud, E. Bevilion, J.L. Yang, G. Dezanneau, Mater. Sci. Eng. B – Advanced Funct. Solid-State Mater. 176 (2011) 1178–1183.
- [17] H. Wang, R.R. Peng, X.F. Wu, J.L. Hu, C.R. Xia, J. Am. Ceram. Soc. 92 (2009) 2623–2629.
- [18] C. Herring, J. Appl. Phys. 21 (1950) 301–303.
- [19] C.B.H. Eva Jud, Ludwig J. Gauckler, J. Am. Ceram. Soc. 88 (2005) 3013–3019.
- [20] S.B.L. Doubova, S. Boldrini, M. Fabrizio, C. Mortabo, C. Pagura, J. Appl. Electrochem. 39 (2009) 2129–2141.
- [21] S. Barison, M. Battaglini, T. Cavallin, S. Daolio, L. Doubova, M. Fabrizio, C. Mortalo, S. Boldrini, R. Gerbas, Fuel Cells 8 (2008) 360–368.
- [22] H.G. Bohn, T. Schober, J. Am. Ceram. Soc. 83 (2000) 768–772.
- [23] S.G.E.I. Ahmed, E. Ahlberg, C.S. .Knee, M. .Karlsson, A. .Matic, Solid State Ionics 177 (2006) 2357–2362.
- [24] H. Iwahara, T. Yajima, T. Hibino, K. Ozaki, H. Suzuki, Solid State Ionics 61 (1993) 65–69.
- [25] H.G. Bohn, T. Schober, J. Am. Ceram. Soc. 83 (2000) 768–772.